New Austalides from the Sponge-Associated Fungus *Aspergillus* sp.

Yaming Zhou,[a] Attila Mándi,[b] Abdessamad Debbab,[a] Victor Wray,[c] Barbara Schulz,[d] Werner E. G. Müller,[e] WenHan Lin,[f] Peter Proksch,[a] Tibor Kurtán,*[b] Amal H. Aly*[a]

[a] Institut für Pharmazeutische Biologie und Biotechnologie, Heinrich-Heine-Universität, Universitätsstrasse 1, Geb. 26.23, D-40225 Düsseldorf, Germany
    Fax: +49 211 81 11923, E-mail: amal.hassan@uni-duesseldorf.de
[b] Department of Organic Chemistry, University of Debrecen, POB 20, 4010 Debrecen, Hungary
    Fax: +36 52 453 836, E-mail: kurtan.tibor@science.unideb.hu
[c] Helmholtz Centre for Infection Research, Inhoffenstraße 7, D-38124 Braunschweig, Germany
[d] Institut für Mikrobiologie, Technische Universität Braunschweig, Spielmannstraße 7, 31806 Braunschweig, Germany
[e] Institut für Physiologische Chemie und Pathobiochemie, Johannes-Gutenberg-Universität, Duesbergweg 6, D-55128 Mainz, Germany
[f] National Research Laboratories of Natural and Biomimetic Drugs, Peking University, Health Science Center, 100083 Beijing, People's Republic of China

Abstract

Chromatographic separation of a crude extract obtained from the fungus *Aspergillus* sp., isolated from the Mediterranean sponge *Tethya aurantium*, yielded five new meroterpenoid metabolites, austalides M-Q (**1-5**), together with nine known compounds (**6-13**). The structures of the new compounds were unambiguously elucidated on the basis of extensive 1D and 2D NMR methods and mass spectral analysis. Furthermore, the absolute configurations of **1** and **4** were determined by TDDFT ECD calculations allowing the assignment of derivatives **2**, **3** and **5** as well. The calculations revealed that the conformation of the benzene-fused phtalide chromophore, sensitive to even minor changes in its proximity, is decisive for the ECD parameters rendering the simple ECD comparison of related homochiral austalides difficult. All compounds were evaluated for their cytotoxic activity against murine cancer cell line L5178Y by the MTT method. Compounds **8** and **11** exhibited

moderate to pronounced cytotoxicity with IC_{50} values of 39.4 and 0.2 μM, respectively, whereas the remaining investigated compounds showed weak or no activity in this assay.

Keywords

Sponge-associated fungi; marine natural products; *Aspergillus*; *Tethya aurantium*; cytotoxicity; TDDFT ECD calculation; chroman chromophore

Introduction

Over the past years, marine microorganisms have proven to be a prolific source of structurally interesting and biologically active natural products. Marine fungi in particular have attracted considerable interest due to the diversity in chemical structures and biological activities observed for their secondary metabolites.[1,2] Bioactive natural products from marine-derived fungi were reported for the first time back in the 1940s from a fungal strain of *Acremonium chrysogenum*, which yielded cephalosporin C, the parent compound of cephalosporin antibiotics.[3] Meanwhile, marine-derived fungi have been isolated from various organisms, including algae, mollusks and particularly sponges.[4,5] Yet, sponge-derived fungi were found to be among the most prolific sources of bioactive compounds.[6]

The genus *Aspergillus* (Moniliaceae) contains approximately 180 species found in various climates worldwide in both terrestrial and marine environments.[7] *Aspergillus* species and their chemical profiles have been studied by numerous research groups. The genus has proven to be a rich source of secondary metabolites with novel structures and interesting bioactivity.[8-12] Examples of isolated metabolites include meroterpenoids,[11,13-15] isochroman derivatives,[10,16-18] drimane sesquiterpenoids,[8,19] and cyclic tripeptides,[12] which exhibited interesting biological activities, such as plant growth inhibition,[16] cytotoxic activity against tumor cell lines,[8,10] selective

2

antifungal activity,[12] as well as inhibition of endothelin-type B receptors.[19]

As part of our ongoing research on marine fungi,[8,20,21] we have investigated a marine-derived fungal *Aspergillus* strain, isolated from a specimen of the Mediterranean sponge *Tethya aurantium*. In this study five new meroterpenoids, named austalides M-Q (**1-5**) (Figure **1**), along with nine known compounds (**6-13**), were isolated. Previously known compounds were identified by comparing their spectroscopic and physical data (^{1}H and ^{13}C NMR, MS and $[\alpha]_D$) with literature values. The structure elucidation of the new metabolites, austalides M-Q (**1-5**), is described in detail. Moreover, all compounds isolated were evaluated for their cytotoxicity against the murine lymphoma cell line L5178Y using the MTT assay.

Results and Discussion

The mycelia and culture medium of the fungus *Aspergillus* sp. were extracted with ethyl acetate. The resulting crude ethyl acetate extract was subjected to repeated column chromatography followed by semi-preparative HPLC separation to obtain five new austalides M-Q (**1-5**) (Figure 1), along with eight known compounds (**6-13**). Based on the spectroscopic data and comparison with data reported in the literature, the known compounds **6-13** (Figure 2) were readily identified as 4-acetyl-3,4-dihydro-6,8-dihydroxy-3-methoxy-5-methylisocoumarine (**6**),[22] 2,3,4-trimethyl-5,7-dihydroxy-2,3-dihydrobenzofuran (**7**),[23] 4-acetyl-3,4-dihydro-6,8-dihydroxy-5-methylisocoumarine (**8**),[24] phenol A acid (**9**),[25] butyrolactone II (**10**),[26,27] methyl-3,4,5-trimethoxy-2-(2-(nicotinamido)benzamido)benzoate (**11**),[28] citrinin (**12**),[29] and dicitrinin A (**13**).[30,31] Compound **11**, previously isolated from *Aspergillus fumigatus* collected from the air and dust of asthmatic patients' rooms,[32] is reported here for the first time from a sponge associated fungus. The new metabolites (**1-5**) were found to be structurally related to the known austalides A-L previously isolated from *Aspergillus ustus*.[13,14]

The molecular formula of **1** was established as $C_{27}H_{36}O_9$ on the basis of the [M+H]$^+$ signal at *m/z* 505.2423 in the HRESIMS. Its UV spectrum showed maxima at λ_{max} 223 and 267 nm characteristic of a substituted phthalide moiety.[14] ^{1}H and ^{13}C NMR spectra (Tables 1 and 3) indicated the presence of eight methyl groups appearing as singlets in the ^{1}H NMR spectrum, including three methoxy groups resonating at δ_H 3.40, 3.50 and 4.13 ppm (CH$_3$-28, -31 and -29, respectively), one aromatic methyl group at δ_H 2.08 ppm (CH$_3$-23), and four aliphatic methyl groups at δ_H 0.90, 1.33, 1.48 and 1.60 ppm (CH$_3$-27, -24, -26 and -25, respectively). In addition, four methylene groups were observed, one of which was attributed to the oxygenated benzylic methylene group at C-1 (δ_H 5.23 ppm, s), as well as three methine groups, two of which are situated on oxygen-bearing carbon atoms as indicated by their chemical shift values at δ_H 4.11 and 4.44 ppm (H-13 and H-22, respectively). The ^{13}C NMR spectrum (Table 3) confirmed the presence of 27 carbon atoms in the structure. Furthermore, the DEPT experiment revealed the presence of 12 quaternary carbon atoms. Analysis of the ^{1}H-^{1}H COSY spectrum of **1** (Table 1, Figure 3) established the presence of three spin systems which included the correlations observed for the methylene protons resonating at δ_H 2.19 and 2.32 ppm (CH$_2$-12) to the deshielded methine group at C-13, and for the methine proton appearing at δ_H 2.50 ppm (H-21) to the deshielded methine group at C-22. Moreover, the correlation between the protons of both methylene groups at C-18 and C-19 verified the third spin system. Interpretation of the HMQC spectrum allowed the assignment of proton signals to the corresponding proton-bearing carbon atoms.

The connection between the different substructures of **1** was determined by inspection of the HMBC spectrum (Table 1, Figure 3). The tertiary methyl group CH$_3$-27 (δ_C 19.2) correlated with the quaternary carbon C-20 (δ_C 39.8), CH$_2$-19 (δ_C 31.4), CH-21 (δ_C 43.6), and an oxygenated quaternary carbon resonating at δ_C 87.7 assigned to C-14. C-14 further correlated with the methyl groups CH$_3$-25 and CH$_3$-26

(δ_C 26.5 and 29.2, respectively), which were found to constitute a geminal dimethyl moiety, as indicated by their correlation with each other as well as with an oxygenated quaternary carbon resonating at δ_C 86.1 (C-15). Furthermore, the methoxy group OCH$_3$-28 (δ_C 49.0) correlated with a highly deshielded quaternary carbon resonating at δ_C 120.3 which was assigned to C-17, in agreement with reported chemical shifts observed for the carbon atom of *ortho* esters.[14] H-21 correlated with C-20, C-22, CH$_3$-27, and an aromatic quaternary carbon at δ_C 119.4 (C-6). The location of OCH$_3$-31 (δ_C 56.4) was established based on its correlation with C-22. H-22 correlated with C-20, C-31, C-6, as well as with three oxygenated quaternary carbons, two aromatic ones overlapping at δ_C 158.9, and an aliphatic one at δ_C 77.3, assigned to C-5, C-7 and C-11, respectively. Correlations of the tertiary methyl group CH$_3$-24 (δ_C 28.8) with C-11, C-21 and CH$_2$-12 (δ_C 43.8) provided the remaining connections of the spin systems previously observed in the ^{1}H-^{1}H COSY spectrum. The methoxy group OCH$_3$-29 (δ_C 63.3) was attached to C-5 as indicated by the respective HMBC correlation. The aromatic CH$_3$-23 (δ_C 10.7) correlated to the quaternary aromatic carbons C-7, C-8 (δ_C 116.2), and C-9 (δ_C 149.3), and hence was placed at C-8. The remaining ^{13}C resonances at δ_C 108.9 and 171.5 were attributed to the remaining sp^2 carbon atom of the completely substituted benzene ring (C-4) and the carbonyl carbon C-3, respectively. This was further confirmed by correlation of C-9 with the oxygenated benzylic methylene group CH$_2$-1 (δ_C 70.0), which in turn correlated with C-4 and C-3.

The relative configuration of **1** was deduced from analysis of the ROESY spectrum. Correlations were observed for CH$_3$-24 to H-21 indicating that rings C and D are *cis*-fused. This was further confirmed by OCH$_3$-31 correlations to H-21 and CH$_3$-24. The correlation observed between CH$_3$-27 and H-22, but not to H-21, indicated a *trans* relationship between CH$_3$-24 and CH$_3$-27. CH$_3$-25 and CH$_3$-27 as well as CH$_3$-26 and H-13 are *cis* oriented based on the correlations observed between

them. Consequently, ring C is *cis*-fused with ring B and *trans*-fused with the seven-membered ring. Thus, the relative stereochemistry of **1** was established as (11S*,13R*,14R*,20R*,21S*,22S*). For the determination of the absolute configuration, the solution ECD spectrum of **1** was recorded in acetonitrile and TDDFT ECD calculation of solution conformers was carried out. The experimental ECD spectrum is dominated by the strong negative Cotton effect (CE) at 217 nm ($\Delta\varepsilon$= 16.00) accompanied by a positive CE at 196 nm ($\Delta\varepsilon$= 5.61) and three weaker transitions at 262, 295 and 301 nm (Figure 4). The MMFF conformational search followed by B3LYP/6-31G(d) DFT reoptimization afforded two conformational isomers (conformer A and B in Figure 5 with 77.2% and 19.5% populations) above 3% population. The two conformers showed minor differences in the orientations of methoxy and hydroxy groups and the conformation of the fused phtalide moiety. In both conformers, the benzylic 22-OMe group adopted axial orientation to relieve the *peri* interaction with the 5-OMe group and the pyran ring of the chroman chromophore had *M* helicity. The weak coupling between H-22 and the contiguous H-21, indicating a torsion angle close to 90° between these vicinal protons,[33] corroborated the axial orientation of the 22-OMe group. In spite of their similarities, the computed ECD spectra of the two conformers were significantly different (Figure SI1 and SI2), *i.e.* the major conformer reproduced well the two intense high-energy CEs, while the minor one seems responsible for the negative CE at 262 nm. The different ECDs of the conformers were attributed to the different orientation of the C-3 carbonyl relatively to the benzene ring ($\omega_{O3,C3,C4,C9}$). The torsional angle $\omega_{O3,C3,C4,C9}$ was found to be –178.8° for the major conformer and +174.3° for the minor one. The Boltzmann-weighted ECD spectra of the two conformers reproduced well the two strong CEs of the high-energy region, which allowed determining the absolute configuration of **1** as (–)-(11S,13R,14R,20R,21S,22S). However, the agreement was quite poor for the weak transitions above 250 nm, which could be

improved by setting the ratio of the two conformers to 1:1 (see Figure SI3). The CD calculation revealed that the $\omega_{O3,C3,C4,C9}$ torsional angle and ratio of the conformers, determined by the central chirality elements, are decisive for the observed CEs, which makes the application of the chroman helicity rule[34] unrelevant.

The absolute configuration of **1** corroborates those determined for austalides A and D by X-ray crystallographic studies.[15,35] However, austalide D has an additional chirality center due to an additional C-19 acetoxy group, and the C-22 chirality center of **1** is missing from both austalides A and D due to the lack of the 22-methoxy substituent.[15,35] Thus, **1** was identified as a new natural product and named as austalide M.

Compound **2** displayed similar spectral data to those of **1** suggesting that both compounds have the same basic molecular framework. HRESIMS indicated the molecular formula $C_{28}H_{36}O_{10}$ in accordance with the $[M+H]^+$ signal at m/z 533.2388, thus revealing a 28 amu increase in the molecular weight compared to **1**. ^{1}H, ^{13}C NMR and DEPT spectra of **2** were similar to those of **1** (Tables 1 and 3) except for the replacement of the benzylic C-22 methoxy group by a methyl ester group resonating at δ_H 2.07 and δ_C 21.3 (CH_3-32). The respective ester carbonyl carbon was detected at δ_C 171.6 (C-31). This was further confirmed by the observed downfield chemical shift of the H-22 signal (δ_H 6.21) caused by the acetyl substituent. Inspection of COSY, HMQC and HMBC spectra (Table 1) indicated that apart from the methyl ester function at C-22, the two compounds were identical. Based on the ROESY spectrum, **2** has (11S*,13R*,14R*,20R*,21S*,22S*) relative configuration in accordance with the corresponding chirality centers of **1**. Accordingly, **2** was finally characterized as a new natural product named austalide N.

The molecular formula of **3** was determined as $C_{26}H_{34}O_9$, from the prominent signal at m/z 491.2293 corresponding to $[M+H]^+$ in the HRESIMS, indicating a loss of 14 amu compared to **1**. Physicochemical data of **3** were almost identical with those

of **1** (Tables 1 and 3) apart from the disappearance of the C-22 methoxy group in the NMR spectra of **3**. This suggested that **3** possesses the same skeleton as **1** but it has a benzylic 22-OH group instead of the 22-OMe, which accounts for the 14 amu molecular weight difference. Accordingly, slight downfield and large upfield shifts were observed for H-22 (δ_H 4.97) and C-22 (δ_C 62.0), respectively, in the ^{1}H and ^{13}C NMR spectra of **3**. As with **2**, further confirmation of the planar structure was achieved by analysis of DEPT, COSY, HMQC and HMBC spectra (Table 1). Moreover, the ROESY spectrum indicated the (11S*,13R*,14R*,20R*,21S*,22S*) relative configuration in agreement with those of **1** and **2**. Hence, **3** was identified as a new natural product and named austalide O.

Compound **4** has the molecular formula of $C_{26}H_{36}O_7$, from the HRESIMS with a prominent peak at m/z 483.2349 [M+Na]$^+$. Its physical characteristics were also comparable to those of **1** suggesting the same basic molecular framework. ^{1}H and ^{13}C NMR spectra of **4** (Tables 2 and 3) indicate the presence of seven methyl groups appearing as singlets in the ^{1}H NMR spectrum, including two methoxy groups resonating at δ_H 3.68 and 4.04 ppm (CH$_3$-28 and -29, respectively), one aromatic methyl group at δ_H 2.08 ppm (CH$_3$-23), and four aliphatic methyl groups at δ_H 0.70, 1.20, 1.19 and 1.27 ppm (CH$_3$-27, -24, -25 and -26, respectively). In addition, six methylene groups were observed, one of which was attributed to the oxygenated benzylic methylene group at C-1 (δ_H 5.21 ppm, s), as well as two methine groups. The ^{13}C NMR spectrum (Table 3) confirmed the presence of 26 carbon atoms in the structure. Furthermore, the DEPT experiment revealed the presence of 11 quaternary carbon atoms. Analysis of the ^{1}H-^{1}H COSY spectrum of **4** (Table 2, Figure 6) established the presence of three spin systems which included the fragment CH$_2$(12)CH$_2$(13)CH(14) based on the correlations observed between the corresponding protons resonating at δ_H 1.61 (CH$_2$-12), 1.52 and 1.83 (CH$_2$-13), as well as 2.14 (H-14) ppm, thus indicating the loss of the hydroxyl group substituent at

C-13 present in **1**-**3** as well as of the oxo-bridge connecting C-14 to C-17. Moreover, the correlation between the protons of methylene groups at C-18 (δ_H 2.32 and 2.60 ppm) and C-19 (δ_H 1.80 and 2.42 ppm), and between the methylene protons appearing at δ_H 2.78 and 3.03 ppm (CH$_2$-22) to the methine group at C-21 (δ_H 1.70 ppm) verified the remaining two spin systems. Proton signals were assigned to their corresponding carbon atoms by analysis of the HMQC spectrum.

The structural units identified in **4** were connected on the basis of correlations observed in the HMBC spectrum (Table 2, Figure 6). The tertiary methyl group CH$_3$-27 (δ_C 19.5) correlated with the quaternary carbon C-20 (δ_C 41.6), CH$_2$-19 (δ_C 34.9), CH-21 (δ_C 41.2), and CH-14 (δ_C 40.1). C-14 further correlated with the methyl groups CH$_3$-25 and CH$_3$-26 (δ_C 28.0 and 33.2, respectively), which were found to constitute a geminal dimethyl moiety, as indicated by their correlation with each other as well as with an oxygenated quaternary carbon resonating at δ_C 75.7 (C-15). The upfield chemical shift of C-15 in **4** compared to that observed in **1**-**3** indicated its location within a side chain and not as part of a seven-membered ring as in **1**-**3**. Furthermore, the methoxy group OCH$_3$-28 (δ_C 52.0) correlated with an ester carbonyl carbon resonating at δ_C 177.7 which was assigned to C-17. H-21 correlated with CH$_2$-19, C-20, CH$_3$-27, CH$_2$-22 (δ_C 18.5), and C-6 (δ_C 118.0). CH$_2$-22 correlated with C-20, CH-21, C-6, as well as with the oxygenated quaternary carbons C-5 (δ_C 158.1), C-7 (δ_C 160.0) and C-11 (δ_C 78.3). Correlations of the tertiary methyl group CH$_3$-24 (δ_C 27.9) with C-11, C-21 and CH$_2$-12 (δ_C 40.2) provided the remaining connections of the spin systems previously observed in the ^{1}H-^{1}H COSY spectrum. The methoxy group OCH$_3$-29 (δ_C 62.1) was attached to C-5 as indicated by the respective HMBC correlation. The aromatic CH$_3$-23 (δ_C 10.6) correlated to the quaternary aromatic carbons C-7, C-8 (δ_C 117.3), and C-9 (δ_C 148.0), and hence was placed at C-8. The remaining ^{13}C resonances at δ_C 108.0 and 172.1 were attributed to C-4 and C-3, respectively. This was further confirmed by correlation of C-9 with CH$_2$-1 (δ_C 69.8),

which in turn correlated with C-8, C-4 and C-3. Accordingly, **4** shows familiar features to **1**-**3** except for that the seven-membered ring of **1**-**3** was opened at the oxo-bridges giving rise to 2 side chains located at C-20 and C-14 instead.

The relative configuration of **4** was established by interpretation of the ROESY spectrum. By analogy with **1**, CH$_3$-24 correlated with H-21 thus denoting *cis*-fusion of rings C and D. This was further confirmed by correlations observed for H-21 with H-14 and CH$_3$-24, indicating the *cis* orientation of H-21 and H-14. A *trans* relationship between CH$_3$-24 and -27 was assumed from the absence of correlations between CH$_3$-27 and H-14, H-21 or CH$_3$-24. Accordingly, the relative stereochemistry of **4** was determined as (11*S**,14*R**,20*S**,21*R**). Compound **4** lacked the benzylic chirality center and its ECD spectrum was completely different from that of **1**, which implied that ECD calculation was required for the configurational assignment. The ECD spectrum of **4** showed four main ECD bands at 267, 228, 212 and 194 nm with alternating negative, positive, negative, positive CEs, respectively (Figure 7). The MMFF conformational search followed by B3LYP/6-31G(d) DFT reoptimization of 31 conformers afforded four conformational isomers with 40.0%, 23.5%, 16.8% and 15.1% populations above 2% populations. Besides slightly different orientations of the side-chains, the value of the torsional angle $\omega_{O3,C3,C4,C9}$ was identified as the main difference among the conformers (Figure 8). In contrast to the situation for austalide M (**1**), the two lowest-energy conformers had positive torsional angle $\omega_{O3,C3,C4,C9}$, while the two higher-energy ones had negative ones. In accordance conformer A and B gave nearly identical calculated ECDs and different from those of conformer C and D, which were similar. The Boltzmann-weighted ECD spectra of (11*R*,14*R*,20*S*,21*R*)-**4** computed with TZVP basis set and three different functionals (B3LYP, BH&HLYP, PBE0) reproduced well the experimental ECD spectrum with PBE0 giving the best agreement (Figure 8). Thus the absolute configuration of **4** was unambiguously determined as (–)-(11*S*,14*R*,20*S*,21*R*) and it was named as austalide P. The ECD

calculation also revealed that the sign of the torsional angle $\omega_{O3,C3,C4,C9}$, *i.e.* the conformation of the benzene-fused pthalide ring, is decisive for the ECD parameters. The major conformers of austalide M (**1**) and P (**4**) had oppositely signed torsional angles $\omega_{O3,C3,C4,C9}$, which resulted in markedly different ECD spectra. The torsional angle $\omega_{O3,C3,C4,C9}$ of the conformers and their populations are clearly determined by the central chirality elements and the benzylic C-22 chirality center has obviously a determining role. The results of the ECD calculation also explain the fact that the ECD spectra (Figure 9) of austalide N (**2**) and O (**3**) were different from that of austalide M (**1**), although they are homochiral and they differ only in the nature of the benzylic C-22 substituent. The nature of the benzylic C-22 substituent (methoxy, acetoxy or hydroxyl) has an effect on the torsional angle $\omega_{O3,C3,C4,C9}$ of the conformers and their populations, which in turn determines the ECD parameters. The examples of austalides suggest that a simple comparison of their ECD spectra, a general procedure for the determination of absolute configuration for structurally related compounds, can not be used safely in the presence of a chirally perturbed benzene-fused phtalide chromophore.

The HRESIMS of **5** exhibited a prominent peak at *m/z* 459.2376 [M+H]$^+$ indicating a molecular formula of $C_{26}H_{34}O_7$. The ^{1}H, ^{13}C NMR and DEPT data of **5** (Tables 2 and 3) were similar to those of **4** apart from the replacement of one of the methylene protons at C-13 by a hydroxyl group in **5**, as evidenced by the chemical shifts of CH-13 (δ_H 4.11, δ_C 72.2). In addition, the hydroxyl group at C-15 of **4** was absent and one of the geminal methyl groups was replaced by an olefinic methylene group, the protons of which resonate downfield at δ_H 4.96 and 5.05 ppm (CH$_2$-25). This was further confirmed by the analysis of the ^{1}H-^{1}H COSY spectrum (Table 2) which verified the fragment CH$_2$(12)CH(13)CH(14) derived from the correlations observed between the methylene protons at δ_H 2.02 and 2.41 ppm (CH$_2$-12), the proton at C-13, and H-14 detected at 2.20 ppm. HMQC and HMBC spectra (Table 2)

gave further evidence for the assigned partial structures of **5**. The correlations observed for CH$_3$-26 (δ_H 1.90) to C-14 (δ_C 54.3), the olefinic quaternary carbon detected at δ_C 148.0 (C-15), and an olefinic methylene carbon at δ_C 116.2 ppm (C-25), confirmed the dehydrogenation of the C-15—C-25 bond in **5** compared to that of **4**. The ROESY spectrum of **5** showed similar correlations to those of **4** indicating (11S*,13R*,14S*,20S*,21R*) relative configuration, which regarding the corresponding chirality centers, was homochiral with that of austalide M (**1**). Since compound **5** exhibited nearly identical ECD spectrum with that of **4** and the C-11 and C-21 chirality centers, the closest ones to the substituted chroman chromophore, were the same, its absolute configuration was determined as (–)-(11S,13R,14S,20S,21R) and it was named austalide Q.

The main structural difference between the new austalides M-Q (**1**-**5**) and previously reported austalides with the same molecular framework is the presence of an additional substituent at C-22 in **1**-**3**, compared to the known austalides A-F.[13,14] Furthermore, austalide P (**4**) lacks a substituent at C-13 having a methylene group in this position, whereas austalide Q (**5**) features a C-15—C25 double bond, compared to the structurally related austalides G and H.[13,14]

Compounds **1**-**13** were evaluated for their cytotoxic activity against the murine cancer cell line L5178Y by the MTT assay.[36] Only compound **8** exhibited pronounced cytotoxicity with an IC$_{50}$ values of 0.2 μM. Compound **11** showed moderate activity (IC$_{50}$ 39.4 μM), whereas the remaining compounds showed weak or no activity in the assay (Table 4).

Experimental Section

General Experimental Procedures: Optical rotations were determined on a Perkin-Elmer-241 MC polarimeter and CD spectra were recorded on a J-810 CD spectropolarimeter. ^{1}H, ^{13}C, and two-dimensional NMR spectra were recorded in

methanol-d_4 on Bruker ARX 400 or Bruker ARX 500 NMR spectrometers. ESIMS was conducted on a Finnigan LCQ Deca mass spectrometer, and HRESIMS spectra were obtained on a FTHRMS-Orbitrap (Thermo-Finnigan) mass spectrometer. Solvents were distilled prior to use, and spectral grade solvents were used for spectroscopic measurements. HPLC analysis was performed using a Dionex P580 system coupled to a photodiode array detector (UVD340S). Routine detection was at 235, 254, 280, and 340 nm. The separation column (125×4 mm, L×i.d.) was prefilled with Eurospher-10 C_{18} (Knauer, Germany), and the following gradient was used (MeOH, 0.02% H_3PO_4 in H_2O): 0 min, 10% MeOH; 5 min, 10% MeOH; 35 min, 100% MeOH; 45 min, 100% MeOH. TLC plates with silica gel F_{254} (Merck, Darmstadt, Germany) were used for monitoring of fractions using dichloromethane/methanol-based solvent systems. Detection was at 254 and 366 nm or by spraying the plates with anisaldehyde reagent.

Fungal material: The sponge *Tethya aurantium*, collected from the Mediterranean Sea near Italy, was surface sterilized by immersing in 70% ethanol for 30 sec followed by rinsing three times in sterilized artificial sea water. Then, the sponge was cleaved aseptically into small segments ($\approx$ 1.5 x 1.5 mm). The material was placed on a potato carrot agar medium and incubated at room temperature (25 °C). After several days hyphae growing from the sponge material were transferred to fresh plates with the same medium, incubated again and periodically checked for culture purity. The fungus was identified as *Aspergillus* sp. (Moniliaceae) using a molecular biological protocol[37] as well as by morphological characterization.

Cultivation: Mass growth of the fungus for the isolation and identification of secondary metabolites was carried out on two different media, namely biomalt agar and spelt barley (composed of 200 g barley, 200 g spelt, 2 g soy protein, 2 mg $MnCl_2$

und 250 mL distilled water) solid media for 21 days at 22 °C. The cultures obtained from both media were then lyophilized, extracted with ethyl acetate, and the dry residues left after evaporation were defatted with petroleum ether.

Extraction and Isolation: The culture media were extracted with ethyl acetate to afford 35 g of dry residue after removal of solvent under reduced pressure. The EtOAc extract was then partitioned between n-hexane and 90% MeOH, the latter yielding 18.0 g dry residue. This residue was subjected to vacuum liquid chromatography (VLC) on silica gel employing a step gradient of dichloromethane/methanol to yield ten fractions (F1-F10). Fraction F2 (1.7 g) was subjected to chromatographic separation using HP-20 with a step gradient of water/methanol to yield **10**. Sub-fractions were chromatographed on Sephadex LH-20 with methanol as eluting solvent. Based on detection by TLC, fractions were combined and subjected to semi-preparative HPLC (Merck, Hitachi L-7100) using a Eurosphere 100-10 C_{18} column (300 × 8 mm, L×i.d.) with an eluting gradient of MeOH/H_2O. Yields of compounds were as follows: **1** 8.5 mg, **2** 8.0 mg, **3** 4.5 mg, **4** 4.5 mg, **5** 1.6 mg, **6** 11.0 mg, **7** 28.0 mg, **8** 7.5 mg, **9** 6.0 mg, **10** 120.0 mg, **12** 1.9 mg, and **13** 4.5 mg. Similarly, fraction F6 (771.6 mg) was chromatographed on Sephadex LH-20 with methanol as eluting solvent followed by semi-preparative HPLC to yield **11** 4.5 mg.

Austalide M (1): brown amorphous solid (MeOH); $[\alpha]^{20}_D$ –43 (c 0.35, MeOH); UV (MeOH/H_2O) λ_{max} 223.7, 267.8 nm; ECD (MeCN), λ [nm] ($\Delta\varepsilon$), $c = 2.1 \times 10^{-4}$): 301 (–0.23), 295 (0.14), 262 (–2.07), 217 (–16.00), 196 (5.61). ^{1}H and ^{13}C NMR data, see Tables 1 and 3; ESIMS positive m/z 504.9 $[M + H]^+$, 527.1 $[M + Na]^+$; HRESIMS m/z 505.2423 $[M + H]^+$ (calc. for $C_{27}H_{37}O_9$, 505.2438).

Austalide N (2): brown amorphous solid (MeOH); $[\alpha]^{20}_D$ –15 (c 0.40, MeOH); UV (MeOH/H_2O) λ_{max} 223.9, 266.9 nm; ECD (MeCN), λ [nm] ($\Delta\varepsilon$), $c = 3.1 \times 10^{-4}$):

300sh (0.15), 284sh (–0.25), 264 (–0.92), 231 (–2.29), 224sh (–2.00), 201 (0.11). ^{1}H and ^{13}C NMR data, see Tables 1 and 3; ESIMS positive m/z 532.8 [M + H]$^+$, 554.9 [M + Na]$^+$; HRESIMS m/z 533.2388 [M + H]$^+$ (calc. for $C_{28}H_{37}O_{10}$, 533.2387).

Austalide O (3): brown amorphous solid (MeOH); [α]$^{20}_D$ –41 (c 0.15, MeOH); UV (MeOH/H$_2$O) λ_{max} 222.8, 268.4 nm; ECD (MeCN), λ [nm] ($\Delta\varepsilon$), c = 3.4 × 10^{-4}): 296 (0.35), 260sh (–1.25), 245 (–1.60), 225sh (1.77), 212 (5.02). ^{1}H and ^{13}C NMR data, see Tables 1 and 3; ESIMS positive m/z 490.8 [M + H]$^+$, 513.1 [M + Na]$^+$; HRESIMS m/z 491.2293 [M + H]$^+$ (calc. for $C_{26}H_{35}O_9$, 491.2281).

Austalide P (4): brown amorphous solid (MeOH); [α]$^{20}_D$ –35 (c 0.15, MeOH); UV (MeOH/H$_2$O) λ_{max} 221.7, 270.1 nm; ECD (MeCN), λ [nm] ($\Delta\varepsilon$), c = 3.6 × 10^{-4}): 295sh (–0.92), 267 (–4.41), 239sh (–1.10), 228 (4.01), 212 (–4.43), 194 (2.28). ^{1}H and ^{13}C NMR data, see Tables 2 and 3; ESIMS positive m/z 460.8 [M + H]$^+$, 483.1 [M + Na]$^+$, 943.0 [2M + Na]$^+$; HRESIMS m/z 461.2532 [M + H]$^+$, 483.2349 [M + Na]$^+$ (calc. for $C_{26}H_{37}O_7$, 461.2539).

Austalide Q (5): brown amorphous solid (MeOH); [α]$^{20}_D$ –40 (c 0.16, MeOH); UV (MeOH/H$_2$O) λ_{max} 220.5, 267.7 nm; ECD (MeCN), λ [nm] ($\Delta\varepsilon$), c = 2.6 × 10^{-4}): 294sh (–0.31), 263 (–2.01), 239sh (–0.37), 226 (2.78), 208 (–1.58), 194 (1.57). ^{1}H and ^{13}C NMR data, see Tables 2 and 3; ESIMS positive m/z 459.0 [M + H]$^+$, 481.1 [M + Na]$^+$, 939.1 [2M + Na]$^+$; HRESIMS m/z 459.2376 [M + H]$^+$, 481.2195 [M + Na]$^+$ (calc. for $C_{26}H_{35}O_7$, 459.2383).

Cell Proliferation Assay: Cytotoxicity was tested against L5178Y mouse lymphoma cells using a microculture tetrazolium (MTT) assay and compared to that of untreated controls as described previously.[38,39] Experiments were repeated three times and carried out in triplicate. As negative controls, media with 0.1% EGMME/DMSO were included in the experiments. The depsipeptide kahalalide F isolated from *Elysia grandifolia*[38] was used as positive control.

Computational section: Conformational searches were carried out by means of the Macromodel 9.7.211[40] software using Merck Molecular Force Field (MMFF) with implicit solvent model for chloroform. Geometry reoptimizations at B3LYP/6-31G(d) level of theory followed by TDDFT calculations using various functionals (B3LYP, BH&HLYP, PBE0) and TZVP basis set were performed by the Gaussian 03[41] package. Boltzmann distributions were estimated from the ZPVE corrected B3LYP/6-31G(d) energies. CD spectra were generated as the sum of Gaussians[42] with 3000 cm^{-1} half-height width (corresponding to ca. 16 nm at 230 nm), using dipole-velocity computed rotational strengths for conformers above 3%. The MOLEKEL[43] software package was used for visualization of the results.

References

[1] M. A. Abdel-Wahab, R. N. Asolkar, P. Inderbitzin, W. Fenical, *Phytochemistry* **2007**, *68*, 1212–1218.

[2] M. E. Rateb, R. Ebel, *Nat. Prod. Rep.* **2011**, *28*, 290–344.

[3] E. P. Abraham, P. B. Loder, *Cephalosporins and penicillins; chemistry and biology*, E. H. Flynn (ed.), Academic Press, New York, **1972**, p. 1-26.

[4] M. P. Lopez-Gresa, N. Cabedo, M. C. Gonzalez-Mas, M. L. Ciavatta, C. Avila, J. Primo, *J. Nat. Prod.* **2009**, *72*, 1348–1351.

[5] G. Bringmann, G. Lang, S. Steffens, K. Schaumann, *J. Nat. Prod.* **2004**, *67*, 311–315.

[6] M. Daferner, T. Anke, O. Sterner, *Tetrahedron* **2002**, *58*, 7781–7784.

[7] J. He, W. E. M. Kithsiri, B. P. Bashyal, J. Zhan, C. J. Seliga, M. X. Liu, E. E. Pierson, L. S. Piesron, H. D. Vanetten, A. A. L. Gunatilaka, *J. Nat. Prod.* **2004**, *67*, 1985–1991.

[8] H. Liu, R. Edrada-Ebel, R. Ebel, Y. Wang, B. Schulz, S. Draeger, W.E.G. Müller, V. Wray, W. Lin, P. Proksch, *J. Nat. Prod.* **2009**, *72*, 1585–1588.

[9] K. Kito, R. Ookura, S. Yoshida, M. Namikoshi, T. Ooi, T. Kusumi, *J. Nat. Prod.* **2007**, *70*, 2022–2025.

[10] Z. Lu, Y. Wang, C. Miao, P. Liu, K. Hong, W. Zhu, *J. Nat. Prod.* **2009,** *72,* 1761–1767.

[11] A. N. Yurchenko, O. F. Smetanina, A. I. Kalinovsky, M. V. Pivkin, P. S. Dmitrenok, T. A. Kuznetsova, *Russ. Chem. Bull.* **2010**, *59*, 852–856.

[12] J. Zheng, Z. Xu, Y. Wang, K. Hong, P. Liu, W. Zhu, *J. Nat. Prod.* **2010,** *73,* 1133–1137.

[13] R.M. Horak, P. S. Steyn, R. Vleggaar, *J. Chem. Soc. Perkin Trans. I* **1985**, 345–356.

[14] R.M. Horak, P. S. Steyn, R. Vleggaar, *J. Chem. Soc. Perkin Trans. I* **1985**, 363–367.

[15] R.M. Horak, P. S. Steyn, P.H. Van Rooyen, R. Vleggaar, *J. Chem. Soc. Chem. Comm.* **1981**, 1265–1267.

[16] H. G. Cutler, F. G. Crumley, J. P. Springer, R. H. Cox, *J. Agric. Food Chem.* **1981**, *29*, 981–983.

[17] J. Kohno, H. Hiramatsu, M. Nishio, M. Sakurai, T. Okuda, S. Komatsubara, *Tetrahedron* **1999**, *55*, 11247–11252.

[18] J. Kohno, M. Sakurai, N. Kameda, M. Nishio, K. Kawano, N. Kishi, T. Okuda, S. Komatsubara, *J. Antibiot.* **1999**, *52*, 913–916.

[19] M. A. Hayes, S. K. Wrigley, I. Chetland, E. E. Reynolds, A. M. Ainsworth, D. V. Renno, M. A. Latif, X.-M. Cheng, D. J. Hupe, P. Charlton, A. M. Doherty, *J. Antibiot.* **1996**, *49*, 505–512.

[20] J. Xu, J. Kjer, J. Sendker, V. Wray, H. Guan, R. A. Edrada, W. H. Lin, J. Wu, P. Proksch, *J. Nat. Prod.* **2009**, *72*, 662–665.

[21] H. B. Liu, R. A. Edrada-Ebel, R. Ebel, Y. Wang, B. Schulz, S. Draeger, W. E. G. Müller, V. Wray, W. H. Lin, P. Proksch, *Helv. Chim. Acta.* **2011**, *94*, 623–631.

[22] K. Krohn, U. Floerke, M. S. Rao, K. Steingroever, H. J. Aust, S. Draeger, B. Schulz, *Nat. Prod. Lett.* **2001**, *15*, 353–361.

[23] C. H. Chen, C. Y. Shaw, C. C. Chen, Y. C. Tsai, *J. Nat. Prod.* **2002**, *67*, 740-741.

[24] D. A. Mulholland, P. Cheplogoi, N. R. Crouch, *Biochem. Sys. Ecol.* **2003**, *31*, 793–797.

[25] R. Thomas, G. Hans, *Liebigs Ann.* **1995**, 885–888.

[26] K. V. Rao, A. K. Sadhukhan, M. Veerender, V. Ravikumar, E. V. S. Mohan, S. D. Dhanvantri, M. Sitaramkumar, J. Moses Babu, K. Vyas, G. Om Reddy, *Chem. Pharm. Bull.* **2000**, *48*, 559–562.

[27] K. Nitta, N. Fujita, T. Yoshimura, K. Aral, Y. Yamamoto, *Chem. Pharm. Bull.* **83**, *31*, 1528–1533.

[28] K. Arai, S. Shimizu, Y. Yamamoto, *Chem. Pharm. Bull.* **1981**, *29*, 1005–1012.

[29] J. Barber, J. L. Cornford, T. D. Haoward, D. *J.* Sharples, *Chem. Soc. Perkin Trans. I* **1987**, 2743–2744.

[30] B. R. Clark, R. J. Capon, E. Lacey, S. Tennant, J. H. Gill, *Org. Biomol. Chem.* **2006**, *4*, 1520–1528.

[31] D. Wakana, T. Hosoe, T. Itabashi, K. Okada, G. M. C. Takaki, T. Yaguchi, K. Fukushima, K. Kawai, *J. Nat. Med.* **2006**, *60*, 279–284.

[32] Y. Yamamoto, K. Nitta, K. Tango, T. Saito, M. Tsuchimuro, *Chem. Pharm. Bull.* **1965**, *13*, 935–941.

[33] M. Karplus, *J. Am. Chem. Soc.* **1963**, *85*, 2870–2871.

[34] S. Antus, T. Kurtán, L. Juhász, L. Kiss, M. Hollósi, Zs. Májer, *Chirality* **2001**, *13*, 493–506.

[35] J. L. M. Dillen, R. M. Horak, V. J. Maharaj, S. F. Marais, R. Vleggaar, *J. Chem. Soc. Chem. Comm.* **1989**, 393–394.

[36] A. H. Aly, R. A. Edrada-Ebel, I. D. Indriani, V. Wray, W. E. G. Mueller, W. H. Lin, P. Proksch, R. Ebel, *J. Nat. Prod.* **2008**, *71*, 972–980.

[37] S. Wang, X. M. Li, F. Teuscher, D. L. Li, A. Diesel, R. Ebel, P. Proksch, B. G..Wang, *J. Nat. Prod.* **2006**, *69*, 1622–1625.

[38] M. Ashour, R. A. Edrada-Ebel, R. Ebel, V. Wray, W. Waetjen, K. Padmakumar, W. E. G. Mueller, W. H. Lin, P. Proksch, *J. Nat. Prod.* **2006**, *69*, 1547–1553.

[39] J. Carmichael, W. G.. Degraff, A. F. Gazdar, J. D. Minna, J. B. Mitchell, *Cancer Res.* **1987**, *47*, 943–946.

[40] MacroModel, Schrödinger LLC, 2009.

http://www.schrodinger.com/Products/macromodel.html

[41] M. J. Frisch, G. W. Trucks, H. B. Schlegel, G. E. Scuseria, M. A. Robb, J. R. Cheeseman, J. A. Montgomery Jr., T. Vreven, K. N. Kudin, J. C. Burant, J. M. Millam, S. S. Iyengar, J. Tomasi, V. Barone, B. Mennucci, M. Cossi, G.. Scalmani, N. Rega, G. A. Petersson, H. Nakatsuji, M. Hada, M. Ehara, K. Toyota, R. Fukuda, J. Hasegawa, M. Ishida, T. Nakajima, Y. Honda, O. Kitao, H. Nakai, M. Klene, X. Li, J. E. Knox, H. P. Hratchian, J. B. Cross, V. Bakken, C. Adamo, J. Jaramillo, R. Gomperts, R. E. Stratmann, O. Yazyev, A. J. Austin, R. Cammi, C. Pomelli, J. W. Ochterski, P. Y. Ayala, K. Morokuma, G. A. Voth, P. Salvador, J. J. Dannenberg, V. G. Zakrzewski, S. Dapprich, A. D. Daniels, M. C. Strain, O. Farkas, D. K. Malick, A. D. Rabuck, K. Raghavachari, J. B. Foresman, J. V. Ortiz, Q. Cui, A. G. Baboul, S. Clifford, J. Cioslowski, B. B. Stefanov, G. Liu, A. Liashenko, P. Piskorz, I. Komaromi, R. L. Martin, D. J. Fox, T. Keith, M. A. Al-Laham, C. Y. Peng, A. Nanayakkara, M. Challacombe, P. M. W. Gill, B. Johnson, W. Chen, M. W. Wong, C. Gonzalez, J. A. Pople, *Gaussian 03, Revision C.02.*, Gaussian Inc., Wallingford CT, **2004**.

[42] P. J. Stephens, N. Harada, *Chirality* **2010**, *22*, 229–233.

[43] U. Varetto, *MOLEKEL 5.4.*, Swiss National Supercomputing Centre: Manno, Switzerland, **2009**.

Table 1. ¹H NMR, COSY and HMBC data (500 MHz, methanol-d_4) of **1-3**, δ in ppm, J in Hz

Position	1 δ_H	COSY	HMBC	2 δ_H	COSY	HMBC	3 δ_H	COSY	HMBC
1	5.23, s		3, 4, 9	5.25, s		3, 9	5.23, s		3, 9
12	2.19, dd (4.3, 15.6)	13		2.17, dd (4.3, 15.6)	13		2.20, dd (4.4, 15.6)	13	
	2.32, dd (2.2, 15.7)			2.33, dd (1.7, 15.7)			2.32, dd (2.1, 15.7)		
13	4.11, dd (2.3, 4.3)	12		4.08, dd (2.1, 4.0)	12		4.09, dd (2.3, 4.3)	12	
18	1.71, brd (8.6)	19		1.57, m	19		1.64, m	19	
	1.98, brd (8.4)			1.83, dt (5.2, 12.9)			1.96, m		
19	1.98, brd (8.4)	18		1.93, dt (6.1, 12.6)	18		1.96, m	18	
	2.06, m			2.45, dd (4.5, 14.2)			2.13, m		
21	2.50, brs	22	6, 20, 22, 27	2.40, brs	22	6, 20, 22, 27	2.48, brs		20, 22, 27
22	4.44, brs	21	5, 6, 7, 11, 20, 31	6.21, brs	21	5, 6, 7, 11, 20, 21,31	4.97, brs		11
23	2.08, s		7, 8, 9	2.10, s		6, 7, 8, 9	2.09, s		8, 9, 7
24	1.33, s		11, 12, 21	1.36, s		11, 12, 14, 21	1.37, s		11, 12, 21
25	1.60, s		14, 15, 26	1.60, s		14, 15, 26	1.60, s		14, 15, 26
26	1.48, s		14, 15, 25	1.46, s		14, 15, 25	1.47, s		14, 15, 25
27	0.90, s		14, 19, 20, 21	0.98, s		14, 19, 20, 21	0.92, s		14, 19, 20, 21
28	3.40, s		17	3.36, s		17	3.38, s		17
29	4.13, s		5	4.06, s		5	4.16, s		5
31	3.50, s		22						
32				2.07, s		6, 31			

Table 2. ^{1}H NMR, COSY and HMBC data (500 MHz, methanol-d_4) of **4** and **5**, δ in ppm, J in Hz

Position	4 δ_H	COSY	HMBC	5 δ_H	COSY	HMBC
1	5.21, s		3, 4, 8, 9	5.21, s		9
12	1.61 dt (3.8, 14.3)	13		2.02, dd (3.9, 15.3) 2.41, dd (2.4, 15.5)	13	
13	1.52, t (10.7) 1.83, m	12, 14	15, 20, 25, 26, 27	4.11, dd (1.7, 4.5)	12, 14	
14	2.14, dd (3.4, 13.7)	13		2.20, d (1.8)	13	
18	2.32, m 2.60, m	19	17, 19	2.36, t (8.0)	19	17, 19
19	1.80, m 2.42, m	18	14, 17, 18, 20, 21	1.65, m	18	
21	1.70, d (8.1)	22	6, 20, 19, 22, 27	1.80, d (7.5)	22	20
22	2.78, dd (8.1, 18.5) 3.03, d (18.6)	21	5, 6, 7, 11, 20, 21	2.87, dd (4.9, 19.3) 2.93, d (18.5)	21	6, 21
23	2.08, s		7, 8, 9	2.08, s		7, 8, 9
24	1.20, s		11, 12, 21	1.25, s		11, 12, 21
25	1.19, s		14, 15, 26	4.96, d (2.8) 5.05, d (1.8)		
26	1.27, s		14, 15, 25	1.90, s		14, 15, 25
27	0.70, s		14, 19, 20, 21	0.86, s		14, 19, 20, 21
28	3.68, s		17	3.67, s		17
29	4.04, s		5	4.05, s		5

Table 3. ^{13}C NMR data (methanol-d_4) of **1-5**, δ in ppm

Position	1^a	2^a	3^a	4^b	5^b
1	70.0	69.9	69.9	69.8	70.7
3	171.5	171.2	172.0	172.1	172.1
4	108.9	108.5	108.8	108.0	108.0
5	158.9	158.4	158.5	158.1	154.7
6	119.4	116.0	116.0	118.0	118.0
7	158.9	159.6	159.2	160.0	160.0
8	116.2	116.4	116.1	117.3	117.3
9	149.3	150.1	149.2	148.0	146.2
11	77.3	77.1	77.1	78.3	79.3
12	43.8	43.7	43.8	40.2	46.6
13	69.9	69.6	70.0	22.4	72.2
14	87.7	87.6	87.6	40.1	54.3
15	86.1	85.1	86.2	75.7	148.0
17	120.3	120.6	120.5	177.7	176.7
18	32.0	32.0	31.8	30.0	29.9
19	31.4	31.6	31.8	34.9	36.0
20	39.8	40.9	40.1	41.6	40.1
21	43.6	46.3	48.0	41.2	40.7
22	72.2	65.3	62.0	18.5	18.9
23	10.7	10.6	10.8	10.6	10.8
24	28.8	28.8	29.2	27.9	27.8
25	26.5	26.4	26.4	28.0	116.2
26	29.2	29.2	29.0	33.2	26.4
27	19.2	19.2	19.0	19.5	20.7
28	49.0	50.1	50.0	52.0	52.4
29	63.3	63.1	62.2	62.1	62.7
31	56.4	171.6			
32		21.3			

^{a} ^{13}C NMR (100 MHz) ^{b} ^{13}C NMR (150 MHz)

Table 4. Results of cytotoxicity assay for the isolated compounds

Compound tested		L5178Y growth inhibition in % (at 10 μg/mL)	IC$_{50}$ (μg/mL)	IC$_{50}$ (μM)
Austalide M	(**1**)	0		
Austalide N	(**2**)	0		
Austalide O	(**3**)	28.0		
Austalide P	(**4**)	16.2		
Austalide Q	(**5**)	41.7		
4-acetyl-3,4-dihydro-6,8-dihydroxy-3-methoxy-5-methylisocoumarin	(**6**)	9.3		
2,3,4-trimethyl-5,7-dihydroxy-2,3-dihydrobenzofuran	(**7**)	9.1		
4-acetyl-3,4-dihydro-6,8-dihydroxy-5-methylisocoumarin	(**8**)	76.9	9.3	39.4
Phenol A acid	(**9**)	0		
Butyrolactone II	(**10**)	49.1		
Methyl 3,4,5-trimethoxy-2-(2-nicotinamidobenzamido)benzoate	(**11**)	100.1	0.1	0.2
Citrinin	(**12**)	35.8		
Dicitrinin A	(**13**)	44.6		
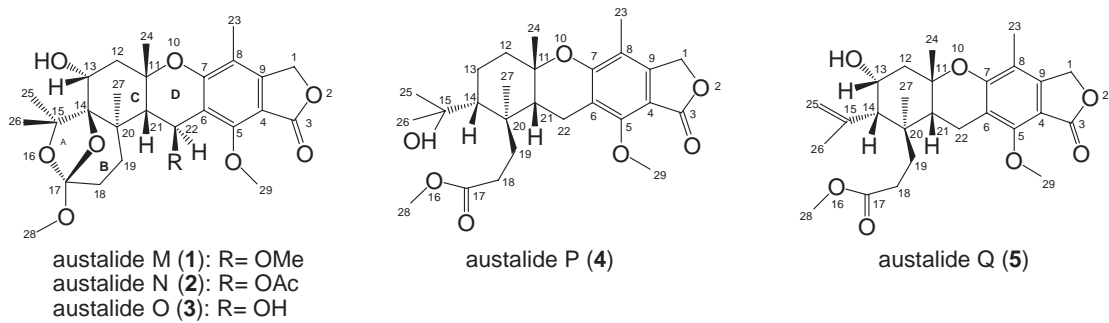
Figure 1. Structures of austalide M-Q (**1-5**) isolated from *Aspergillus* sp.
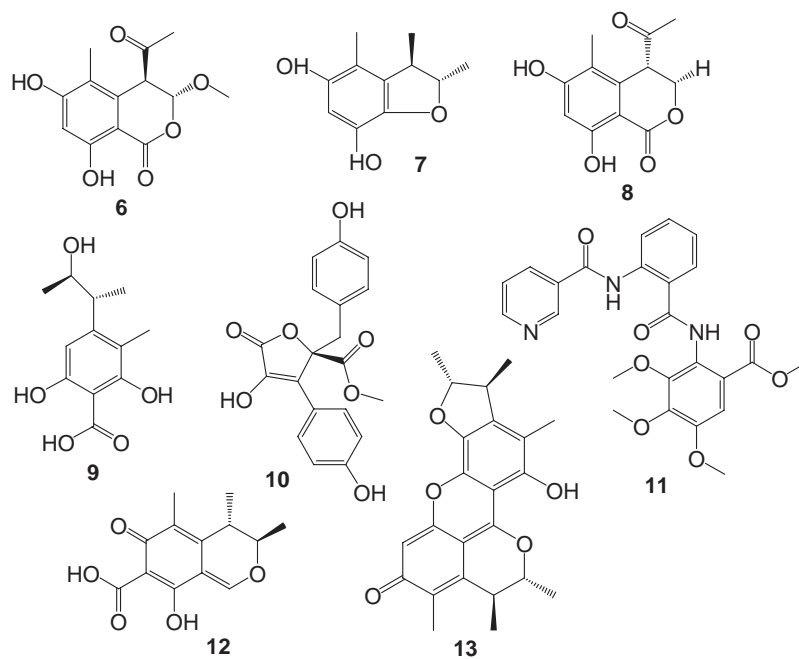
**Figure 2.** Known compounds (**6-13**) isolated from *Aspergillus* sp.
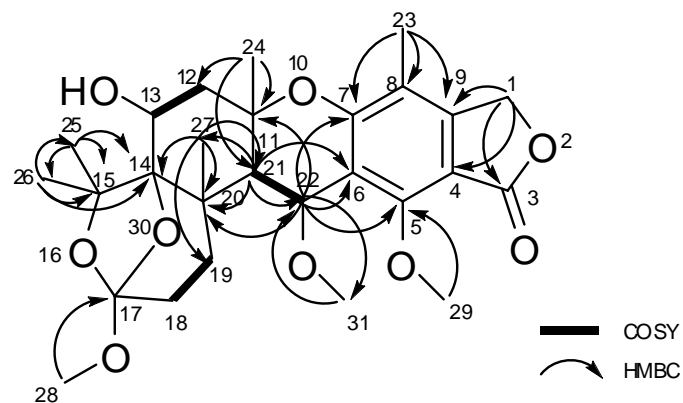
Figure 3. HMBC and ^{1}H-^{1}H COSY correlations of **1**
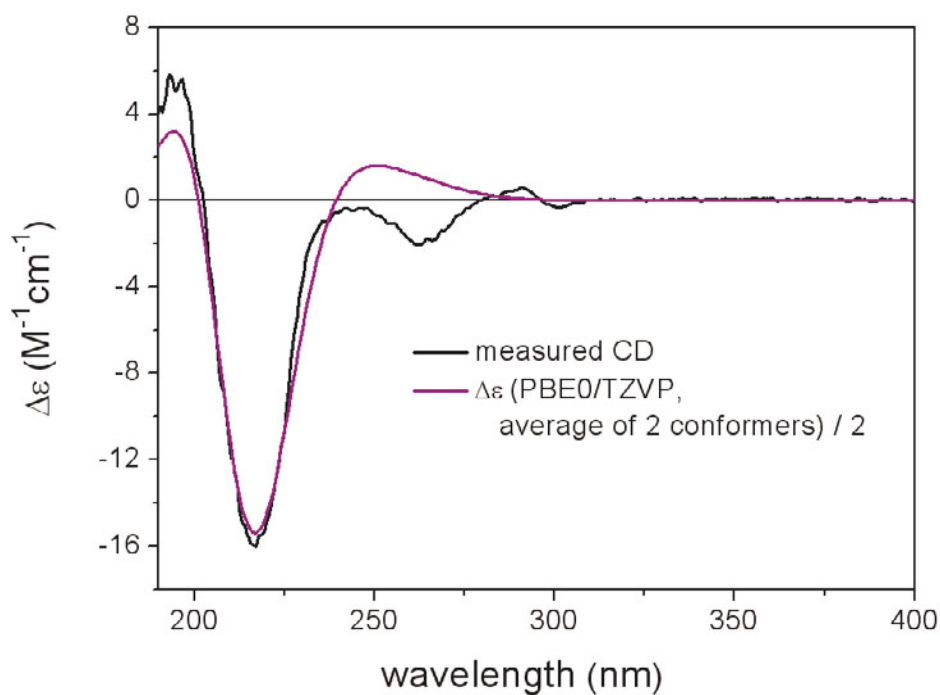
Figure 4. Experimental ECD spectrum of **1** in acetonitrile compared with the Boltzmann-weighted PBE0/TZVP spectrum calculated for the two lowest-energy conformers of the (11*S*,13*R*,14*R*,20*R*,21*S*,22*S*)-enantiomer
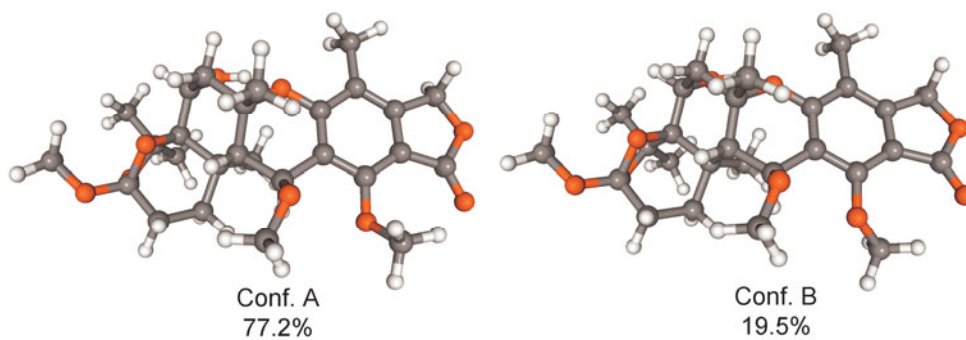
Figure 5. DFT optimized geometries of the two lowest-energy conformers of (11*S*,13*R*,14*R*,20*R*,21*S*,22*S*)-**1** with torsional angle $\omega_{O3,C3,C4,C9}$ −178.8° and +174.3°, respectively
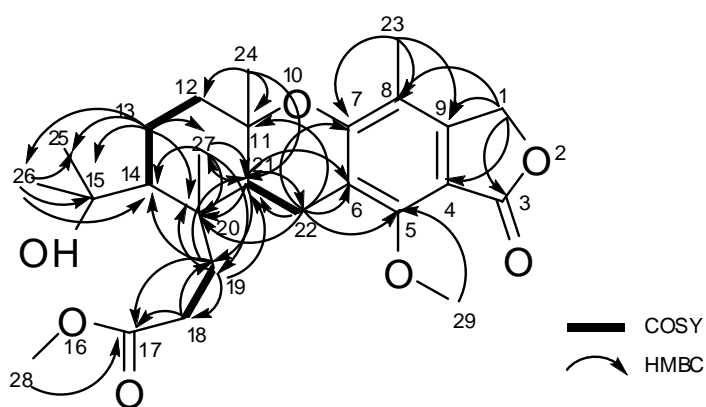
Figure 6. HMBC and ^{1}H-^{1}H COSY correlations of **4**
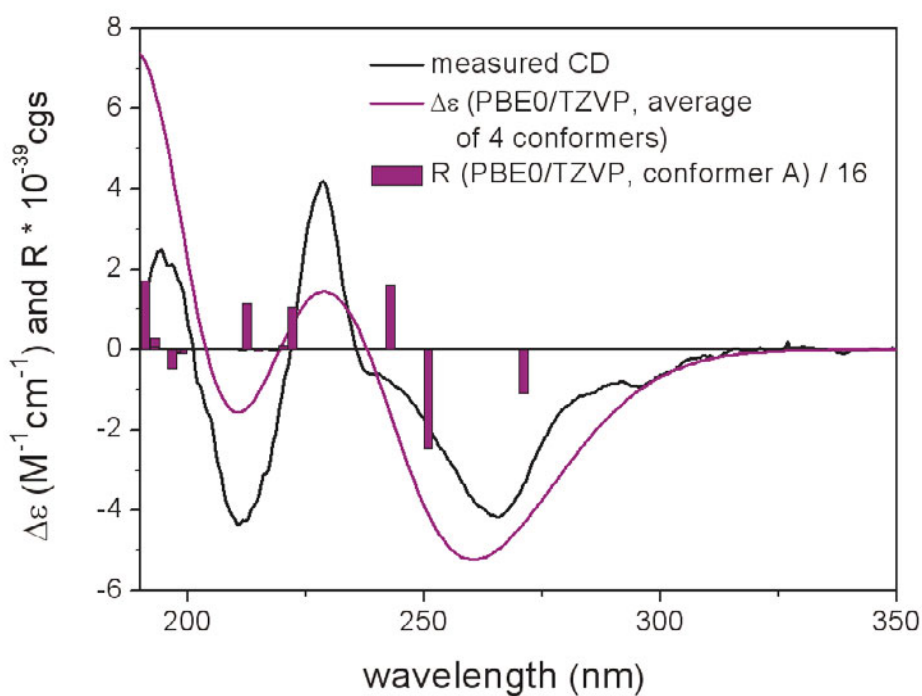
Figure 7. Experimental ECD spectrum of **4** in acetonitrile compared with the Boltzmann-weighted PBE0/TZVP spectrum calculated for the four lowest-energy conformers with (11*S*,14*R*,20*S*,21*R*) absolute configuration. Bars represent rotational strengths (R) of the lowest-energy conformer (40.0%)
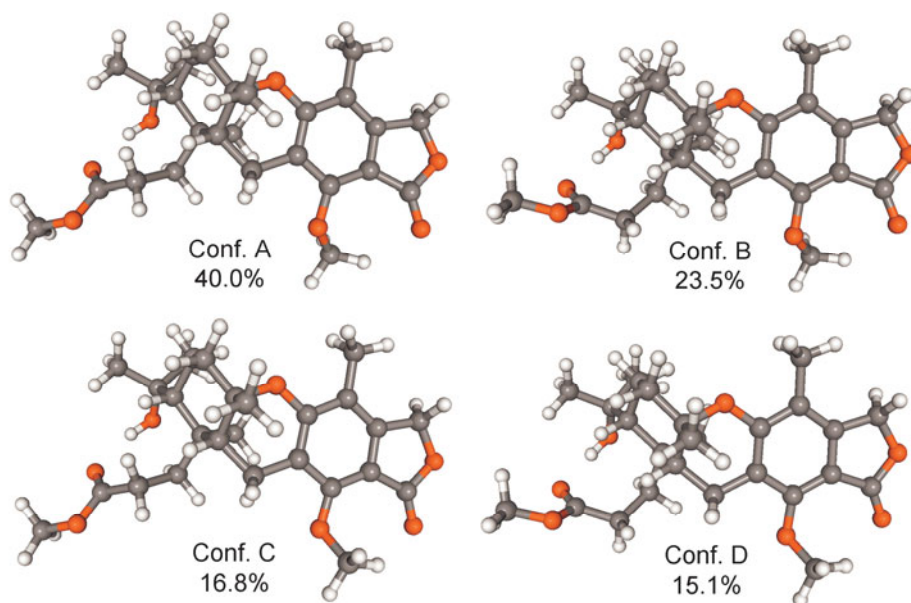
Figure 8. DFT optimized geometries and populations of the four lowest-energy conformers of (11*S*,14*R*,20*S*,21*R*)-**4** with torsional angle $\omega_{O3,C3,C4,C9}$ +174.61°, +174.92°, −176.28° and −175.94°, respectively
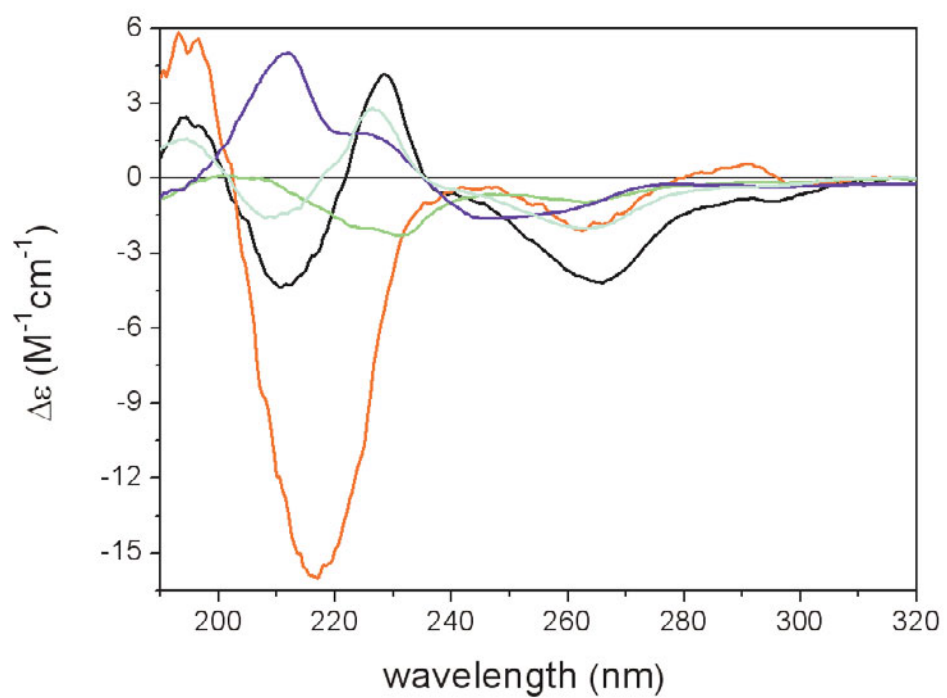
Figure 9. Experimental ECD spectra of austalide M (**1**, red), austalide N (**2**, green), austalide O (**3**, blue), austalide P (**4**, black) and austalide Q (**5**, cyan) in acetonitrile
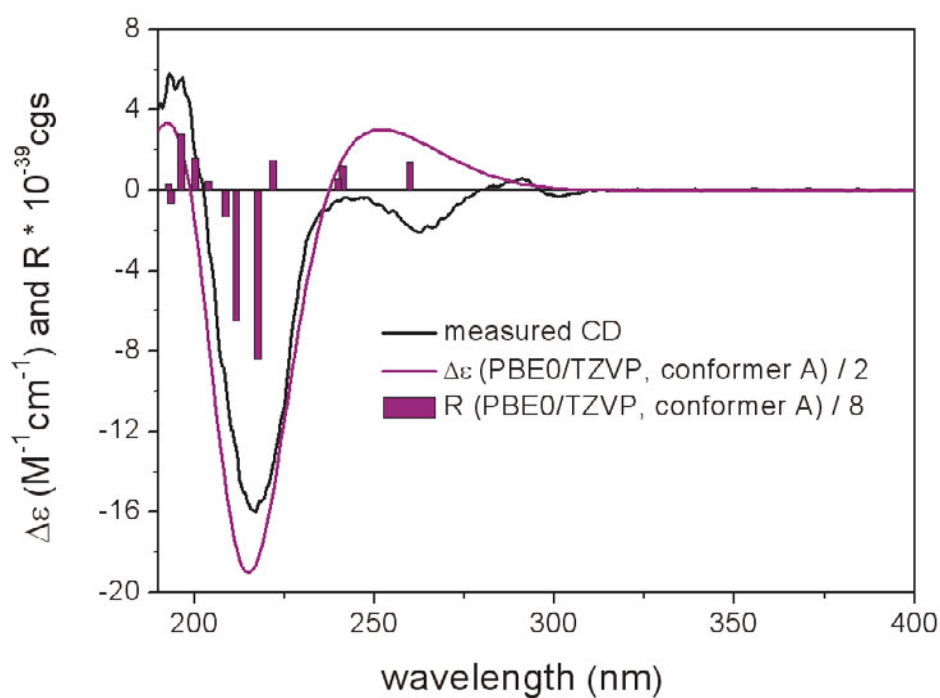
Figure SI1. Experimental ECD spectrum of **1** compared with the PBE0/TZVP spectrum of the lowest-energy (11*S*,13*R*,14*R*,20*R*,21*S*,22*S*)-conformer (conformer A, 77.2% population). Bars represent rotational strengths (R)
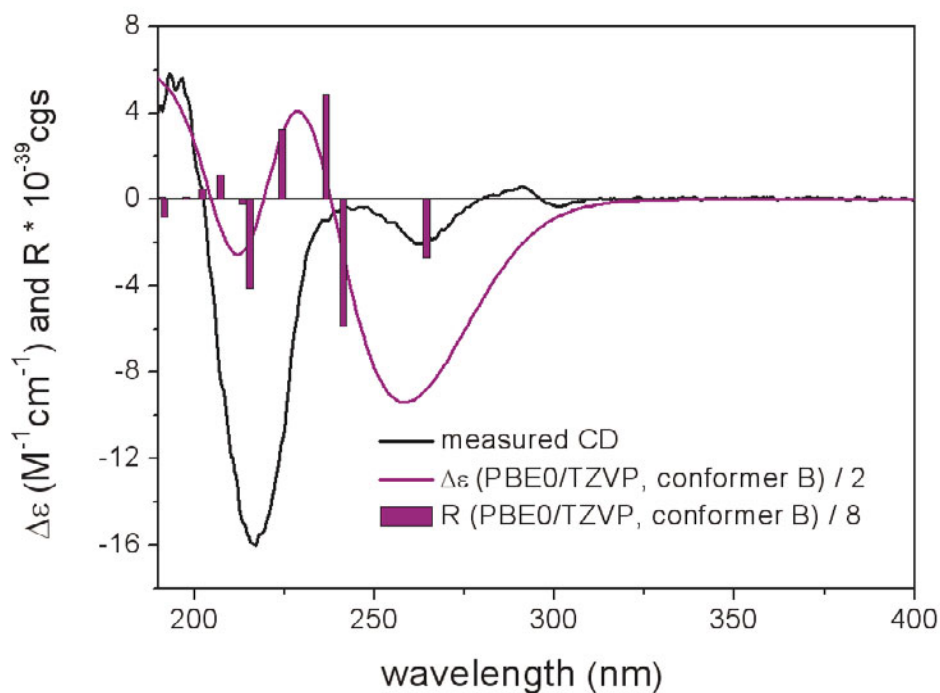
Figure SI2. Experimental ECD spectrum of **1** compared with the PBE0/TZVP spectrum of (11*S*,13*R*,14*R*,20*R*,21*S*,22*S*)-conformer B (19.5% population). Bars

represent rotational strengths (R)
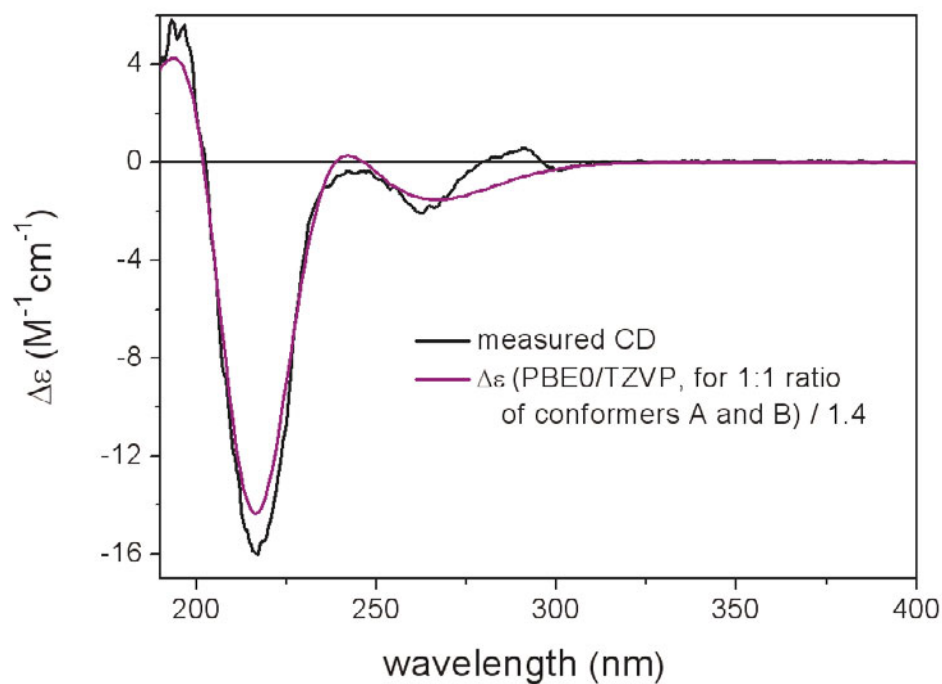
Figure SI3. Experimental ECD spectrum of **1** compared with the PBE0/TZVP spectrum of the two lowest-energy (11*S*,13*R*,14*R*,20*R*,21*S*,22*S*)-conformers supposing their 1:1 ratio